British Journal of Pharmacology (2004) 142, 1273–1280
www.nature.com/bjp

Cellular actions of somatostatin on rat periaqueductal grey neurons *in vitro*

[1]Mark Connor, [1]Elena E. Bagley, [1]Vanessa A. Mitchell, [2]Susan L. Ingram, [1]MacDonald J. Christie, [3]Patrick P.A. Humphrey & [1,*]Christopher W. Vaughan

[1]Pain Management Research Institute, Northern Clinical School, The University of Sydney at Royal North Shore Hospital, E25 NSW 2006, Australia; [2]Department of Psychology, WSU-Vancouver, Vancouver WA 98686, U.S.A. and [3]Theravance Inc., 901 Gateway Blvd, South San Francisco, CA 94080, U.S.A.

Functional studies indicate that the midbrain periaqueductal grey (PAG) is involved in the analgesic actions of somatostatin; however, the cellular actions of somatostatin in this brain region are unknown. In the present study, whole-cell patch clamp recordings were made from rat PAG neurons *in vitro*. In 93% of acutely isolated neurons, somatostatin inhibited Ca^{2+}-channel currents. This effect was mimicked by the sst-2 selective agonist BIM-23027, but not by the sst-1 and sst-5 selective agonists CH-275 and L-362855. In brain slices, 81% of neurons responded to somatostatin (300 nM) with an increase in K^+ conductance that reversed polarity at −114 mV. A greater proportion of somatostatin-sensitive neurons (93%) than somatostatin-insensitive neurons (53%) responded to the opioid agonist met-enkephalin (10 μM). Somatostatin also reduced the amplitude of evoked $GABA_A$-mediated inhibitory postsynaptic currents (IPSCs). The actions of somatostatin in brain slices were mimicked by BIM-23027, but not by CH-275. Somatostatin had a variable effect on the rate of spontaneous miniature IPSCs in normal external potassium solutions. In high external potassium solutions, somatostatin reduced the rate of miniature IPSCs in all neurons, and this inhibition was abolished by addition of Cd^{2+} (30 μM). Somatostatin had no effect on the amplitude of miniature IPSCs. These results indicate that somatostatin acts *via* sst-2 receptors to directly inhibit a subpopulation of PAG neurons by activating a potassium conductance and inhibits GABA release within PAG *via* a presynaptic Ca^{2+}-dependent mechanism. Thus, like opioids, somatostatin has the potential to exert pre- and postsynaptic disinhibitory effects within the PAG.
British Journal of Pharmacology (2004) **142,** 1273–1280. doi:10.1038/sj.bjp.0705894

Keywords: Somatostatin; opioid; analgesia; periaqueductal grey; potassium current; calcium current; synaptic transmission

Abbreviations: ACSF, artificial cerebrospinal fluid; PAG, periaqueductal grey; RVM, rostral ventromedial medulla

Introduction

The peptide somatostatin is widely distributed throughout the central and peripheral nervous system, as well as endocrine tissue, and produces many neural and hormonal actions (Schindler *et al*., 1996). Somatostatin and a number of analogues have analgesic activity in acute (Sandkuhler *et al*., 1990; Eschalier *et al*., 1991; Chapman & Dickenson 1992; Helyes *et al*., 2000; Carlton *et al*., 2001) and chronic inflammatory/neuropathic pain models (Corsi *et al*., 1997; Heppelmann & Pawlak, 1997; Helyes *et al*., 2001; Pinter *et al*., 2002). However, these studies have examined the analgesic actions of somatostatin only at the level of the peripheral nociceptor and within the spinal cord.

The midbrain periaqueductal grey (PAG) forms part of a descending analgesic pathway, which projects *via* the rostral ventromedial medulla (RVM) to modulate nociceptive neurotransmission within the dorsal horn of the spinal cord (Fields & Basbaum, 1999). The PAG is a major site of the analgesic actions of μ-opioids. It has also been demonstrated that microinjection of somatostatin into the PAG and RVM produces analgesia (Helmchen *et al*., 1995). While the cellular actions of opioids within the PAG are well characterized (Chieng & Christie, 1994; Kim *et al*., 1997; Vaughan & Christie 1997a; Connor & Christie 1998), the actions of somatostatin within the PAG are unknown. The present study examined the cellular actions of somatostatin in rat PAG neurons *in vitro*.

Methods

Sprague–Dawley rats (16–40 days old) of either sex were anaesthetized with halothane, decapitated and coronal midbrain PAG slices (250–300 μm) were cut in ice-cold artificial cerebrospinal fluid (ACSF), as described previously (Vaughan & Christie 1997a). The slices were maintained at 34°C in a submerged chamber containing ACSF equilibrated with 95% O_2 and 5% CO_2. For experiments on synaptic currents and postsynaptic K^+ currents, the slices were then transferred to a chamber and superfused continuously (1.8 ml min^{-1}) with ACSF (32°C) of composition: (mM): NaCl, 126; KCl, 2.5; NaH_2PO_4, 1.4; $MgCl_2$, 1.2; $CaCl_2$, 2.4; glucose, 11; $NaHCO_3$, 25. In Cd^{2+} experiments, NaH_2PO_4 was removed for the period of recording. PAG neurons were visualized using infrared Nomarski optics on an upright microscope (Olympus BX50). For experiments on postsynaptic currents in brain

*Author for correspondence; E-mail: chrisv@med.usyd.edu.au
Advance online publication: 19 July 2004

slices, a K^+-gluconate-based internal solution was used, which contained (mM): K-gluconate 95, KCl 30, NaCl 15, $MgCl_2$ 1, HEPES 10, EGTA 11, MgATP 2, NaGTP 0.25. For experiments on synaptic currents, a CsCl-based internal solution was used, which contained (mM): CsCl 140, EGTA 10, Hepes 5, $CaCl_2$ 2, and MgATP 2 (pH 7.3, osmolarity 270–290 mosmoll^{-1}). Voltage clamp recordings (holding potential −60 mV) were made in the whole-cell configuration using an Axopatch 200B (Axon Instruments, Foster City, CA, U.S.A.) with patch clamp electrodes (2–5 MΩ). Series resistance (<20 MΩ) was compensated by 80% and continuously monitored during experiments. Liquid junction potentials of –10 mV for K-gluconate and –4 mV for CsCl based internal solutions were corrected.

In experiments on postsynaptic currents, recordings were filtered (500 Hz low-pass filter) and sampled (1 kHz) for analysis (Axograph 4, Axon Instruments). In experiments on synaptic currents, inhibitory postsynaptic currents (IPSCs) were filtered (1 kHz low-pass filter) and sampled (5 kHz) for analysis (Axograph 4). In some experiments on synaptic currents, electrically evoked (eIPSCs) were elicited in neurons *via* a theta glass stimulating electrode placed 50–200 μm from the recording electrode (rate 0.05–0.1 Hz, stimuli: 5–30 V, 0.01–0.5 ms). In the other experiments on synaptic currents, spontaneous miniature IPSCs (mIPSCs) were obtained in neurons in the presence of TTX (300 nM). Miniature IPSCs above a preset threshold (4.5–5.5 standard deviations above baseline noise) were automatically detected by a sliding template algorithm (Axograph 4), then manually checked offline. Plots of detected event frequency *versus* time and cumulative probability distributions of event amplitudes and interevent intervals were constructed.

For experiments on postsynaptic Ca^{2+} currents, cells were dissociated as previously described (Connor & Christie 1998). Slices were transferred to a dissociation buffer of composition (mM): Na_2SO_4 82, K_2SO_4 30, HEPES 10, $MgCl_2$ 5, glucose 10, containing 20 U ml^{-1} papain, pH 7.3 and incubated for 2–3 min at 35°C. The slices were then placed in fresh dissociation buffer containing 1 mg ml^{-1} bovine serum albumin (BSA) and 1 mg ml^{-1} trypsin inhibitor and the PAG was subdissected out with a fine tungsten wire. Cells were dissociated from the slices by gentle trituration, plated onto plastic culture dishes and kept at room temperature in dissociation buffer. Whole-cell patch clamp recordings of calcium channel currents were made at room temperature (22–24°C). Immediately prior to recording, dishes of cells were superfused with a buffer of composition (mM): NaCl 140, KCl 2.5, $CaCl_2$ 2.5, $MgCl_2$ 1.5, HEPES 10, glucose 10, pH 7.3 in order to wash off the dissociation buffer. For recordings of Ba^{2+} currents through calcium channels (I_{Ca}), cells were perfused in solution containing (mM): tetraethyl ammonium chloride 140, $BaCl_2$ 4, $MgCl_2$ 1, CsCl 2.5, HEPES 10, glucose 10, pH 7.3. Whole-cell patch clamp recordings were made with an intracellular solution containing (mM): CsCl 130, MgATP 5, Na_2GTP 0.2, EGTA 10, $CaCl_2$ 2, NaCl 5, and HEPES 10, pH 7.3. Series resistance (~3 MΩ) was compensated by 80% and continuously monitored during experiments. Leak current was subtracted on line using a P/8 protocol, typically the leak conductance was of the order of 100 pS. I_{Ca} evoked by stepping the membrane potential from a holding potential of −90 mV were filtered (2 kHz low-pass filter) and sampled (5–10 kHz) for later analysis (PCLAMP, Axograph 3; Axon Instruments). Cells were exposed to drugs *via* a series of flow pipes positioned above the cells. The inhibition by drugs was quantified by measuring the current amplitude isochronically with the peak of the control I_{Ca}.

Stock solutions of all drugs were diluted to working concentrations using ACSF immediately before use and applied by superfusion. Met-enkephalin (methionine-enkephalin), bicuculline methiodide, strychnine hydrochloride, bovine serum albumin (BSA), and trypsin inhibitor (Type II-O) were obtained from Sigma (Sydney, Australia); tetrodotoxin (TTX) from Alomone (Jerusalem, Israel). Papain was from Worthington Biochemical Corporation (Freehold, NJ, U.S.A.). BIM-23027 (c[N-Me-Ala-Try-D-Trp-Lys-Abu-Phe])) and L-362855 (c[Aha-Phe-Trp-D-Trp-Lys-Thr-Phe] where Aha is 7-amino heptanoic acid) were a kind gift of Dr P.P.A. Humphrey (Glaxo Institute for Applied Pharmacology, Cambridge, U.K.), CH-275 (des-$AA^{1,2,5}$[$DTrp^8$,$Iamp^9$]-somatostatin) was a kind gift from Drs C. Hoeger and J. Rivier (The Salk Institute, La Jolla, CA, U.S.A.). All pooled data were expressed as means ± s.e.m., and statistical comparisons were made using Student's paired, or unpaired *t*-tests and χ^2 tests for proportions. Dose response curves were constructed using a logistic function (Kaleidograph 3; Synergy Software, Reading, U.S.A.).

Results

Somatostatin increases a K^+-current in a subpopulation of PAG neurons

In brain slices, superfusion of somatostatin (300 nM) produced an outward current (25 ± 2 pA) in 81% ($n = 88/108$) of neurons tested (Figure 1a and b). The μ/δ-opioid agonist met-enkephalin (10 μM) produced an outward current in a greater proportion of neurons that responded to somatostatin (93%, $n = 74/80$), than in neurons that did not respond to somatostatin (53%, $n = 9/17$; $\chi^2 = 17.8$, $P < 0.0001$) (Figure 1a and b). The met-enkephalin current in somatostatin-sensitive and -insensitive neurons was 31 ± 3 and 28 ± 6 pA, respectively ($P > 0.05$). Subsequent application of the $GABA_B$ agonist baclofen (10 μM) produced an outward current in all somatostatin-responding neurons (47 ± 6 pA, $n = 48$) and in all somatostatin-nonresponding neurons (35 ± 3 pA, $n = 17$), which was reversed by the $GABA_B$ antagonist CGP-55845 (1 μM, Figure 1a and c).

The selective sst-2 receptor agonist BIM-23027 (100–300 nM) produced an outward current (18 ± 2 pA) in 90% ($n = 19/21$) of neurons tested (Figure 1c). The selective sst-1 receptor agonist CH-275 (300 nM) was usually without effect (Figure 1c), producing an outward current (9 ± 3 pA) in a smaller percentage of neurons (11%, $n = 2/18$; $\chi^2 = 25$, $P < 0.0001$).

In neurons that responded to somatostatin with an outward current at −60 mV, the resting membrane conductance showed inward rectification with slope conductances of 3.5 ± 0.6 and 5.2 ± 0.8 nS when measured between −60/−90 and −110/−130 mV, respectively ($n = 13$). Somatostatin increased the slope conductances to 3.9 ± 0.5 and 6.1 ± 1.0 nS, when measured over the same potentials (Figure 1d, $n = 13$). ME increased the slope conductances to 4.2 ± 0.7 and 6.1 ± 1.2 nS, when measured over the same potentials ($n = 8$). The

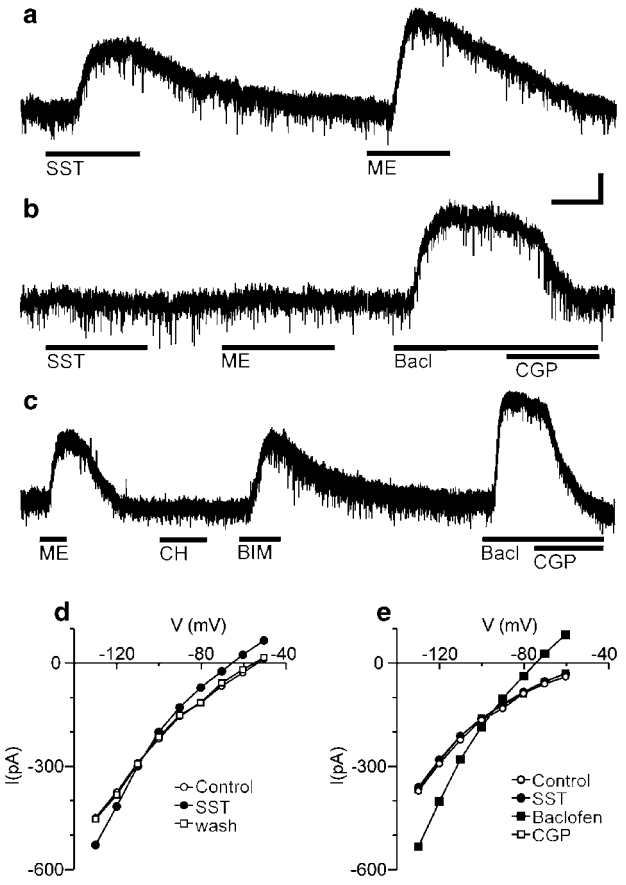

Figure 1 Activation of somatostatin-2 receptors increases a potassium conductance in a subpopulation of mainly μ-opioid-sensitive PAG neurons. Representative raw current traces of somatostatin (a)-sensitive and (b) -insensitive PAG neurons during superfusion of somatostatin (300 nM, SST), met-enkephalin (10 μM, ME), baclofen (10 μM, Bacl), and CGP55845 (1 μM, CGP). (c) Raw current trace of a neuron during superfusion of CH-275 (300 nM, CH) and BIM-23027 (300 nM, BIM). The current–voltage relationships for (d) somatostatin-sensitive and (e) somatostatin-insensitive neurons before (control) and during superfusion of somatostatin (300 nM), baclofen (10 μM), and CGP55845 (1 μM, CGP). Membrane currents were evoked by voltage command steps in 10 mV increments from $-50/-60$ mV to -130 mV (250 ms duration). (a–e) are from five different neurons that were voltage clamped at -60 mV. The vertical scale bar is 20 pA for (a–c) and the horizontal scale bar is 40 s for (a) and (b), and 2 min for (c).

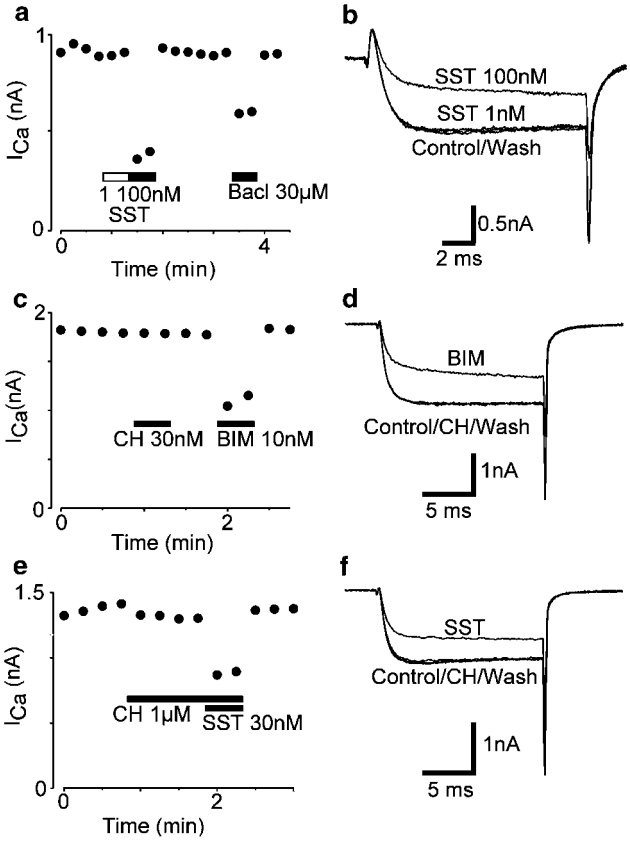

Figure 2 Somatostatin inhibits Ca^{2+} channel currents in PAG neurons. (a, c, e) Time plots of the peak amplitude of I_{Ca} during the application of somatostatin (SST), baclofen (Bacl), CH-275 (CH), and BIM-23027 (BIM). (b, d, f) Example of raw current traces of I_{Ca} for the time plots in (a), (c), (e), respectively. I_{Ca} was elicited by repetitively stepping the membrane potential of a PAG neuron from -90 to 0 mV every 30 s. (a, b) and (c, d) and (e, f) are taken from three different neurons.

somatostatin- and met-enkephalin-induced currents reversed polarity at -114 ± 4 mV ($n=13$) and -114 ± 4 mV ($n=8$), respectively. The slope conductances of neurons, which did not respond to somatostatin, were 3.6 ± 0.8 and 5.9 ± 1.2 nS before and 3.7 ± 0.9 and 5.8 ± 1.2 nS during somatostatin superfusion ($-60/-90$ and $-110/-130$ mV, respectively; Figure 1e, $n=4$). In these neurons, baclofen increased the slope conductances to 5.9 ± 1.8 and 9.7 ± 2.5 nS, when measured over the same potentials (Figure 1e, $n=4$). The baclofen-induced current reversed polarity at -106 ± 6 mV ($n=4$).

Somatostatin inhibits calcium currents in PAG neurons

To record I_{Ca}, acutely isolated PAG neurons were voltage clamped at -90 mV in Na^+- and K^+-free external solution. I_{Ca} in most cells began to activate at test potentials above -40 mV and was invariably greatest at membrane potentials between -10 and 0 mV (Connor & Christie 1998). Somatostatin inhibited I_{Ca} in 93% of PAG neurons ($n=76/82$) tested (Figure 2a and b). The inhibition of I_{Ca} by somatostatin reversed on washout. A concentration–response relationship for somatostatin inhibition of PAG I_{Ca} was determined by application of one or more concentrations of somatostatin to cells stepped repetitively from -90 to 0 mV (Figure 3). Desensitization of the inhibition of I_{Ca} by somatostatin was not observed during brief applications of somatostatin at concentrations less than 30 nM. A logistic function fitted to the concentration–response relationship for somatostatin inhibition of I_{Ca} gave a pEC_{50} 8.2 ± 0.1 and a Hill slope for the curve of 1.1 ± 0.1. The maximum inhibition of I_{Ca} by somatostatin was 38%.

The sst-2 selective agonist BIM-23027 also inhibited I_{Ca} in most PAG neurons (Figure 2c and d, $n=30/33$), with a pEC_{50} of 8.7 ± 0.05 and a Hill slope of 1.3 ± 0.1 (Figure 3). The maximum inhibition of I_{Ca} by BIM-23027 was also 38%. The sst-1 receptor agonist CH-275 (30 nM-1 μM, $n=12$) did not inhibit I_{Ca} in any cell, nor did it affect the inhibition of I_{Ca} by somatostatin (Figure 2c–f). Somatostatin (30 nM) inhibited I_{Ca} by 36 ± 6% in the continued presence of CH-275 (1 μM, $n=5$),

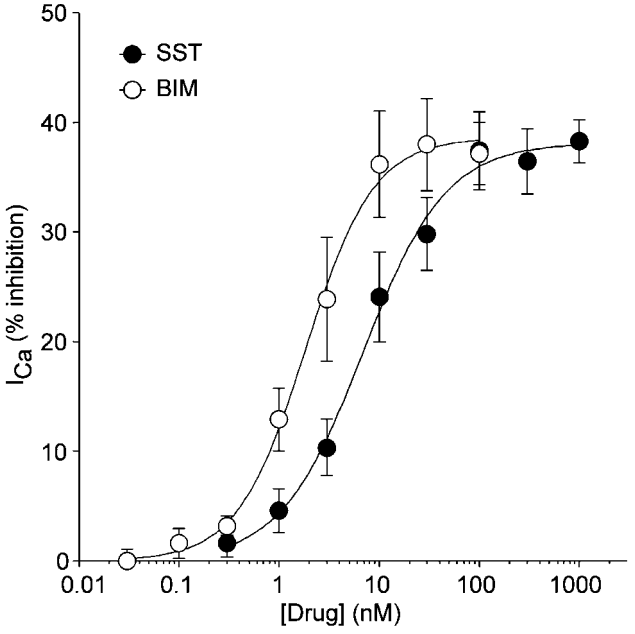

Figure 3 Somatostatin inhibition of Ca^{2+} channel currents is concentration dependent. Concentration–response relationships of somatostatin (SST, filled circles) and BIM-23027 (BIM, open circles) inhibition of Ca^{2+} channel currents (I_{Ca} in isolated cells) in PAG neurons. Each point shows the mean (±s.e.m.) of responses of several different neurons ($n=6$–9). A logistic function was fitted to determine the EC_{50}.

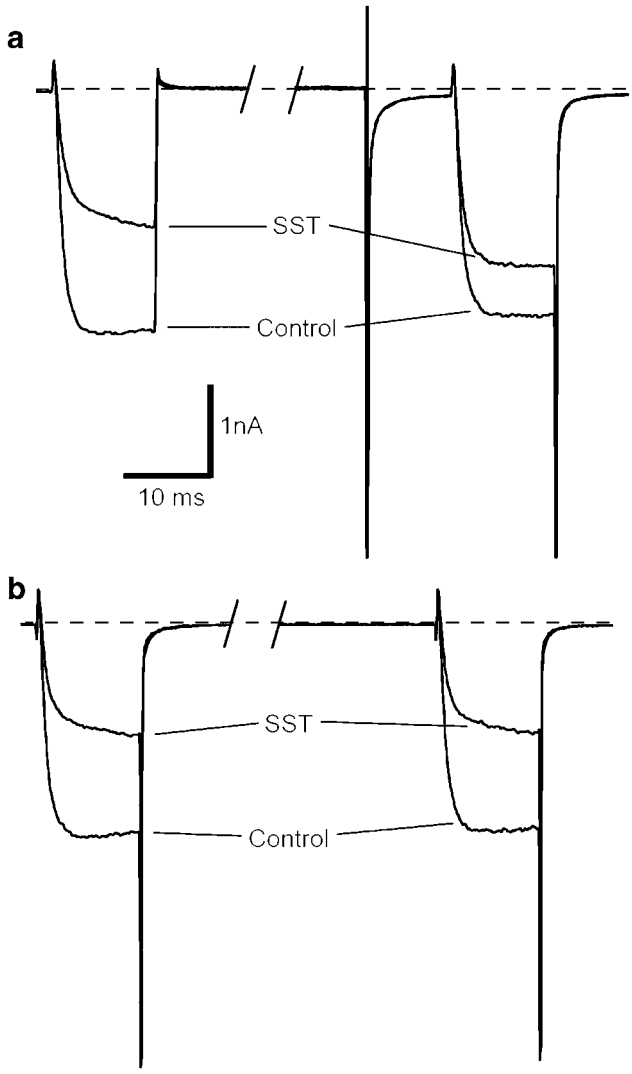

Figure 4 Somatostatin inhibition of I_{Ca} in PAG neurons is relieved by a positive conditioning step. PAG neurons were voltage clamped at −90 mV and stepped twice to a test potential of 0 mV, with 90 ms between the test steps. In (a) an 80 ms conditioning step to + 60 mV was applied to the cell immediately after the first test step and the cell was returned to −90 mV 10 ms before the second test step. In (b) the cell was held at −90 mV between the two test steps. The raw current traces for steps in the absence and presence of somatostatin (SST, 100 nM) are shown, with a section of the trace between the test pulses removed for clarity. The traces were not leak subtracted, and the zero current level is shown by the dashed line. (a) and (b) are each representative of six cells.

while in parallel experiments somatostatin inhibited I_{Ca} by 36±4% ($n=7$). The sst-5 receptor agonist L-362 855 (1 μM) had no effect on I_{Ca} (3±1% inhibition, $n=7$).

The inhibition of I_{Ca} by somatostatin was evident over a range of membrane potentials and was characterized by a significant slowing of the activation of I_{Ca} (Figure 4, Table 1, see below). The inhibition of I_{Ca} by somatostatin could also be attenuated by a strong positive depolarizing step shortly before the test step. In these experiments, cells were stepped twice to 0 mV, with an 80 ms depolarizing step to + 60 mV between the test steps (Figure 4a). In control conditions, the amplitude of the first (T1) step was always larger than the second (T2), but this difference was not statistically significant (Table 1, $P>0.05$, unpaired t test, $n=6$). In the presence of maximally effective concentrations of somatostatin (30–100 nM), T1 was inhibited by 47±3%, while T2 was inhibited by 20±2%. The inhibition of T2 by somatostatin was significantly less than the inhibition of T1 by somatostatin ($P<0.0001$, unpaired t test, $n=6$), and in the presence of somatostatin the amplitude of T2 was significantly greater than that of T1 (Table 1, $P<0.005$, $n=6$). Superfusion of somatostatin caused a 2.5-fold increase in the 0–95% rise time of T1 (Table 1), but an insignificant change in the 0–95% rise time of T2 (Table 1). If there was no step to + 60 mV between T1 and T2 (Figure 4b), there was no difference in the amount somatostatin inhibited T1 and T2 (42±4 *versus* 41±4%, $P>0.05$, unpaired t-test, $n=6$), nor was there any difference in the somatostatin-induced slowing of the rise time between T1 and T2 (Table 1).

Pretreatment of PAG neurons with pertussis toxin (PTX, 500 ng ml^{-1}, 8 h, 35°C) abolished the effects of somatostatin on I_{Ca}. The I_{Ca} of PTX-treated cells in the presence of somatostatin (100 nM) was 98±4% ($n=4$) of the predrug current. In cells from the same animals incubated for 8 h at 35°C in the absence of PTX, somatostatin (100 nM) inhibited I_{Ca} by 37±8% ($n=3$).

Somatostatin inhibits GABAergic synaptic transmission

Electrical stimulation in the presence of CNQX (3 μM) and strychnine (3 μM) elicited evoked IPSCs (eIPSCs) in PAG neurons that were abolished by the $GABA_A$ antagonist bicuculline (30 μM) or picrotoxin (100 μM, Figure 5a). Superfusion of somatostatin (300 nM) had a variable effect on the amplitude of eIPSCs, producing inhibition in a subpopulation

Table 1 Effects of a depolarizing conditioning step on SST modulation of I_{Ca} in PAG neurons

	Control	*SST*
With conditioning step		
Ratio T2 : T1 amplitude	0.87±0.02	1.35±0.05*
0–95% rise time of T1 (ms)	2.0±0.2	5.1±0.7*
0–95% rise time of T2 (ms)	2.3±0.2	2.6±0.1#
Without conditioning step		
Ratio T2 : T1 amplitude	0.97±0.01	0.99±0.01
0–95% rise time of T1 (ms)	2.3±0.2	4.6±0.7**
0–95% rise time of T2 (ms)	2.3±0.2	5.1±0.8**

PAG neurons were stepped twice from −90 to 0 mV, with or without an 80 ms conditioning step to +60 mV preceding the second step (see Figure 4). T1 and T2 are the currents produced by the first and second test steps, respectively. The mean ratio of T2 : T1 (T2/T1) is shown before (control) and during somatostatin (SST, 30–100 nM). With the conditioning step, the SST-induced inhibition of T2 was reduced (increase in T2 : T1). Without the conditioning step, the amplitude of T1 and T2 were similar. * denotes $P<0.005$ between control and SST (paired t-test); ** Denotes $P<0.02$, between control and SST (paired t-test). # Denotes $P<0.005$ between T1 and T2 in the same condition (unpaired t-test).

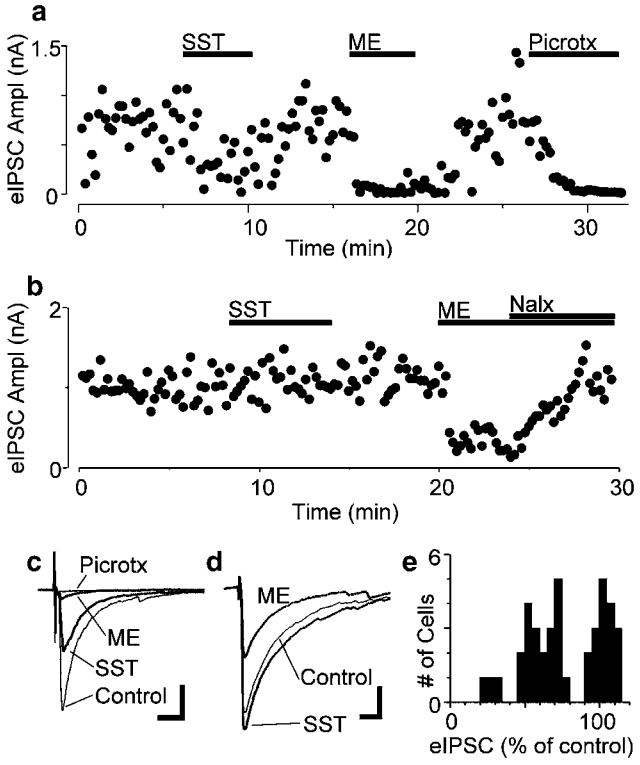

Figure 5 Somatostatin inhibits evoked GABAergic synaptic currents in PAG. Time course of the amplitude of evoked IPSCs in representative somatostatin (a)-sensitive and (b) -insensitive neurons during application of somatostatin (300 nM, SST), met-enkephalin (10 μM, ME), naloxone (1 μM, Nalx), and picrotoxin (100 μM, Picrotx). (c) and (d) are averaged raw traces of evoked IPSCs from before (Control) and during somatostatin, met-enkephalin and picrotoxin for neurons depicted in (a) and (b), respectively. (e) Histogram of the inhibition of the evoked IPSCs produced by somatostatin (300 nM) in all neurons tested (expressed as a percentage of control predrug amplitude). (a–d) are taken from two neurons in the presence of CNQX (3 μM) and strychnine (3 μM), voltage clamped at −60 mV. The scale bars for (c) and (d) are 0.2 nA and 10 ms.

of PAG neurons (Figure 5, range = 20–112% of control, $n=40$). On average, the amplitude of eIPSCs in the presence of somatostatin was 77±4% of control ($P>0.05$). In 57% ($n=23/40$) of PAG neurons, somatostatin reduced the amplitude of eIPSCs by greater than 20% (mean = 57±3% and range = 20–79% of control, Figure 5a, c, e). In the other 43% ($n=17/40$) of PAG neurons, somatostatin reduced the amplitude of eIPSCs by less than 10% (mean = 103±2% and range = 91–112% of control, Figure 5b, d, e). Met-enkephalin (10 μM) reduced the amplitude of eIPSCs in all somatostatin-responding (mean = 30±10% and range = 7–42% of control, $n=5$) and somatostatin-nonresponding (mean = 39±3% and range = 26–47% of control, $n=8$) neurons that were tested (Figure 5).

Superfusion of BIM-23027 (300 nM), but not CH-275 (300 nM) reduced the amplitude of eIPSCs in a subpopulation of PAG neurons (data not shown). On average, the amplitude of eIPSCs in the presence of BIM-23027 and CH-275 was 79±12% (range = 34–118%, $n=6$) and 104±2% (range = 94–113%, $n=7$) of control, respectively.

Somatostatin inhibits GABAergic synaptic transmission via a presynaptic Ca^{2+}-dependent process

To determine whether somatostatin inhibits $GABA_A$-mediated synaptic transmission by a presynaptic reduction in the probability of GABA release, or by a reduction in postsynaptic $GABA_A$ receptor sensitivity, we examined the effect of somatostatin on spontaneous miniature IPSCs (mIPSCs). In the presence of CNQX (3 μM), strychnine (3 μM) and TTX (300 nM), mIPSCs that were blocked by bicuculline (30 μM) or picrotoxin (100 μM) were readily observed. In normal external K^+ concentrations ($[K^+]_{ext}=2.5$ mM), mIPSCs had a mean amplitude of 54±6 pA and a mean rate of 2.5±0.5 s^{-1} ($n=16$). Superfusion of somatostatin (300 nM) had a variable effect on the rate of mIPSCs (range = 44–116% of control, $n=16$). On average, the rate of mIPSCs in the presence of somatostatin was 87±7% of control (Figure 6, $P>0.05$). In contrast, met-enkephalin (10 μM) reduced the rate of mIPSCs in all PAG neurons tested (range = 27–75% of control), on average reducing the mIPSC rate to 51±4% of control (Figure 6, $n=16$, $P<0.05$). Somatostatin and met-enkephalin had no significant effect on the amplitude (98±5% and 92±3% of control, $P>0.05$) and the kinetics of mIPSCs (data not shown).

The inhibition of eIPSCs in PAG neurons may have been due to presynaptic inhibition of voltage-dependent calcium currents that were activated during action potential evoked

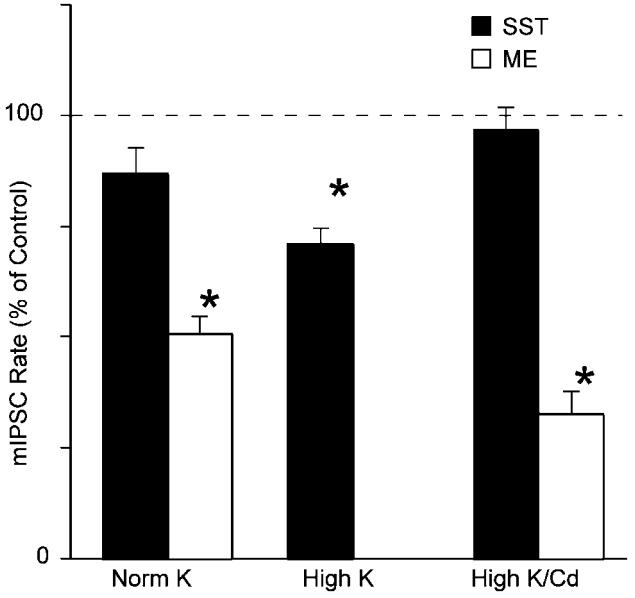

Figure 6 Effect of somatostatin and met-enkephalin on miniature IPSC rate. Bar chart depicting the average effect of somatostatin (300 nM, SST, filled bars) and met-enkephalin (10 μM, ME, open bars) on the rate of mIPSCs (expressed as a percentage of the control predrug rate) in normal potassium (Norm K, 2.5 mM), high potassium (High K, 17.5 mM), and high potassium/Cd^{2+} (High K/Cd; 17.5 mM: 30 μM) external solutions. * Denotes significantly different to control predrug rate ($P<0.05$).

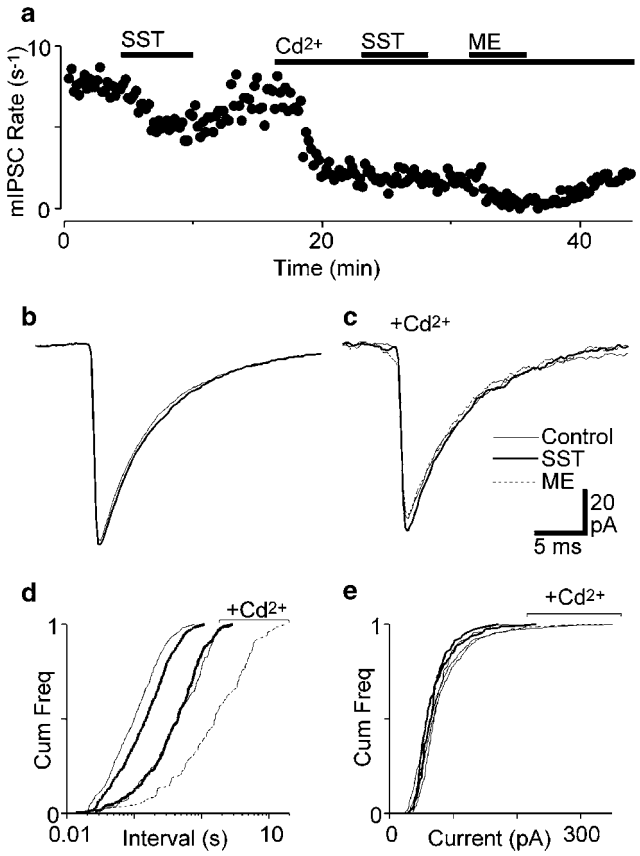

Figure 7 Somatostatin inhibition of GABAergic synaptic transmission is dependent on presynaptic calcium entry. (a) Representative time course of miniature IPSC rate during superfusion of somatostatin (300 nM, SST) and met-enkephalin (10 μM, ME) in a high K^+-containing solution (17.5 mM), then after addition of Cd^{2+} (30 μM). Averaged raw traces of miniature IPSCs before (Control) and during superfusion of somatostatin and met-enkephalin in the (b) absence and (c) presence of Cd^{2+}. Cumulative distribution plots of the (d) interevent interval and (e) amplitude of miniature IPSCs before, then during somatostatin and met-enkephalin, in the presence and absence of Cd^{2+}. (a–e) are taken from one neuron, voltage clamped at -60 mV in the presence of CNQX (3 μM), strychnine (3 μM), and TTX (300 nM).

release, but were relatively inactive during Na^+-channel-independent (TTX-resistant) spontaneous release. We therefore examined the effect of somatostatin (300 nM) on spontaneous mIPSCs during tonic activation of voltage-dependent calcium currents in high external K^+ concentrations ($[K^+]_{ext} = 17.5$ mM). In high external K^+ concentrations, mIPSCs had a mean rate and amplitude of $6.0 \pm 1.1\ s^{-1}$ and 65 ± 8 pA, respectively ($n = 13$). Under these conditions, somatostatin reduced the rate of mIPSCs to $68 \pm 4\%$ of control (Figure 6, range = 45–86%, $n = 13$, $P < 0.001$). Somatostatin had no effect on the amplitude ($95 \pm 3\%$ of control, $P > 0.05$) and kinetics of mIPSCs (Figure 7).

In high external K^+ concentrations, addition of Cd^{2+} (30 μM) reduced the mean rate and amplitude of mIPSCs to 51 ± 8 and $81 \pm 7\%$ of control, respectively (Figure 7, $n = 6$). In high K^+/Cd^{2+}-containing external solutions, somatostatin did not significantly affect the rate of mIPSCs (mean = $97 \pm 5\%$ of control, $n = 11$, $P > 0.05$), even when somatostatin reduced the mIPSC rate prior to addition of Cd^{2+} (Figure 7). In contrast, met-enkephalin reduced the mIPSC rate to $33 \pm 5\%$ of control in high K^+/Cd^{2+}-containing external solutions (Figure 6, 7; $n = 11$, $P < 0.005$). Under these conditions, somatostatin and met-enkephalin had no effect on the amplitude (97 ± 4 and $98 \pm 6\%$ of control, respectively, $P > 0.05$) and kinetics of mIPSCs (Figure 7).

Discussion

The present study demonstrates that somatostatin has pre- and postsynaptic inhibitory actions on rat PAG neurons in a manner consistent with activation of sst-2 receptors. Somatostatin increased a potassium conductance and inhibited calcium channel conductances in the majority of PAG neurons. Somatostatin also inhibited GABAergic synaptic transmission within the PAG *via* a presynaptic calcium-dependent mechanism. These observations suggest that somatostatin might produce analgesia by partly similar disinhibitory mechanisms to μ-opioids within the PAG.

The actions of somatostatin are mediated by five G protein-coupled receptors that can be divided into two pharmacologically distinct groups, namely SST_1 (sst-2, sst-3, and sst-5 receptors) and SST_2 (sst-1 and sst-4 receptors) groups (Hoyer *et al*., 1995). Immunohistochemical studies have demonstrated the presence of sst-1, sst-2A, and sst-3 within the PAG (Dournaud *et al*., 1996; Schindler *et al*., 1997; Hervieu & Emson, 1998). The actions of somatostatin observed in the present study were likely to be mediated by the sst-2 receptor subtype because the observed effects of somatostatin on K^+-

and Ca^{2+}-currents and on evoked GABAergic synaptic currents were mimicked by the sst-2 receptor agonist BIM-23027, but not by the sst-1 and sst-5 receptor agonists CH-275 and L-362855 (e.g. see Selmer *et al*., 2000).

Somatostatin modulated postsynaptic potassium and calcium conductances in PAG neurons. The outward current produced by somatostatin was the result of an increase in an inwardly rectifying potassium conductance (K_{ir}), as has been demonstrated for μ-opioids and nociceptin/orphaninFQ (N/OFQ) in the PAG (Chieng & Christie, 1994; Vaughan *et al*., 1997b, c). Like met-enkephalin, somatostatin activated a conductance that was greater at more negative potentials and had a reversal potential similar to the Nernst potential predicted for a potassium conductance (−106 mV). The inhibition of I_{Ca} in acutely isolated PAG neurons by somatostatin was probably mediated by activation of heterotrimeric guanine nucleotide binding proteins (G proteins). Firstly, the inhibition of I_{Ca} by somatostatin was abolished by pretreatment of the PAG neurons with PTX, which inactivates Gi/Go-type G proteins by catalysing ADP-ribosylation of the α subunit of the G protein heterotrimer. Similar findings have been reported previously with μ-opioid, ORL1, and $GABA_B$ receptors in isolated PAG neurons (Kim *et al*., 1997; Connor & Christie 1998). Secondly, the inhibition of I_{Ca} by somatostatin was associated with a pronounced slowing of the activation of the I_{Ca} and could be significantly reduced by a depolarising prepulse to +60 mV, both characteristic features of the ubiquitous G protein $\beta\gamma$-subunit-mediated pathway for inhibition of I_{Ca} (Herlitze *et al*., 1996; Ikeda, 1996; Zamponi & Snutch, 1998). The present study utilized Ba^{2+} as the external charge carrier for calcium channel currents and an internal solution with strong Ca^{2+} buffering. Thus, these experiments would have been unlikely to detect somatostatin modulation of I_{Ca} *via* Ca^{2+}-dependent processes, which may occur *in vivo*.

Somatostatin inhibited $GABA_A$-mediated evoked IPSCs in a subpopulation of PAG neurons as previously demonstrated for N/OFQ (Vaughan *et al*., 1997b). This differs in comparison with μ-opioids and CB1 cannabinoids that inhibit evoked IPSCs in all PAG neurons (Vaughan & Christie 1997a; Vaughan *et al*., 2000). μ-Opioid and CB1 cannabinoid agonists are thought to inhibit GABAergic synaptic transmission *via* a presynaptic mechanism because they reduce the rate of spontaneous miniature IPSCs, but have no effect on their amplitude, or kinetics. In the present study, somatostatin reduced the rate of spontaneous miniature IPSCs, although this effect was variable as observed previously for N/OFQ (Vaughan *et al*., 1997b). In contrast, somatostatin reduced the rate of miniature IPSCs in the majority of PAG neurons under conditions where presynaptic calcium channels were activated by elevating the external potassium concentration, and this inhibition was abolished by blockade of calcium entry with Cd^{2+}. These observations indicate that somatostatin inhibits transmitter release from GABAergic terminals in PAG by reducing presynaptic calcium entry, or by modulating part of the release process directly dependent on Ca^{2+} influx. Thus, somatostatin differs from μ-opioids and CB1 cannabinoid agonists that inhibit GABA release *via* calcium-entry-independent presynaptic processes in PAG (Vaughan & Christie 1997a; Vaughan *et al*., 1997c; 2000). However, under the right conditions, somatostatin has the potential to inhibit GABAergic synaptic transmission in the majority of PAG neurons, like μ-opioids and CB1 cannabinoids. Variability in the modulation of evoked and miniature IPSCs by somatostatin may be due to heterogeneity in the calcium sensitivity of GABA release from individual nerve terminals in the PAG, rather than heterogeneity in the distribution of presynaptic sst-2 receptors. Alternatively, elevated external potassium concentrations might unmask a subpopulation of low-probability release terminals, which are sensitive to somatostatin.

Functional studies have demonstrated that, like μ-opioids, microinjection of somatostatin into PAG produces analgesia (Helmchen *et al*., 1995). μ-Opioids are thought to activate a descending antinociceptive pathway from the PAG by reducing inhibitory GABAergic influences (disinhibition) on projection neurons (Fields & Basbaum, 1999). Indirect electrophysiological evidence suggests that opioid disinhibition occurs by inhibition of GABAergic interneurons and presynaptic inhibition of transmitter release from GABAergic terminals onto projection neurons (Osborne *et al*., 1996; Vaughan & Christie 1997a). In the present study, it was observed that the pre- and postsynaptic actions of somatostatin partly overlap those of μ-opioids within PAG. Firstly, somatostatin inhibits the majority of μ-opioid-sensitive neurons (putative GABAergic interneurons), but only half of the μ-opioid-insensitive neurons. Secondly, somatostatin inhibits $GABA_A$-mediated synaptic transmission in most neurons, albeit *via* a different presynaptic mechanism to μ-opioids. These observations suggest that somatostatin and μ-opioids produce analgesia by at least partly similar disinhibitory mechanisms in the PAG, as opposed to trigeminal primary afferent neurons where they act upon distinct cell populations (Taddese *et al*., 1995).

This study was supported by National Health & Medical Research Council of Australia grants to C.W.V. (# 153844) and to M.C. (# 153911). We thank Drs C. Hoeger and J. Rivier from The Salk Institute, La Jolla, CA, for the kind gift of CH-275.

References

CARLTON, S.M., DU, J., DAVIDSON, E., ZHOU, S. & COGGESHALL, R.E. (2001). Somatostatin receptors on peripheral primary afferent terminals: inhibition of sensitized nociceptors. *Pain,* **90,** 233–244.

CHAPMAN, V. & DICKENSON, A.H. (1992). The effects of sandostatin and somatostatin on nociceptive transmission in the dorsal horn of the rat spinal cord. *Neuropeptides,* **23,** 147–152.

CHIENG, B. & CHRISTIE, M.J. (1994). Hyperpolarization by opioids acting on μ-receptors of a sub-population of rat periaqueductal gray neurones *in vitro*. *Br. J. Pharmacol.,* **113,** 121–128.

CONNOR, M. & CHRISTIE, M.J. (1998). Modulation of calcium channel currents of acutely dissociated rat periaqueductal grey neurons. *J. Physiol. (London),* **509,** 47–58.

CORSI, M.M., TICOZZI, C., NETTI, C., FULGENZI, A., TIENGO, M., GAJA, G., GUIDOBONO, F. & FERRERO, M.E. (1997). The effect of somatostatin on experimental inflammation in rats. *Anesth. Analg.,* **85,** 1112–1115.

DOURNAUD, P., GU, Y.Z., SCHONBRUNN, A., MAZELLA, J., TANNENBAUM, G.S. & BEAUDET, A. (1996). Localization of the somatostatin receptor SST2A in rat brain using a specific anti-peptide antibody. *J. Neurosci.,* **16,** 4468–4478.

ESCHALIER, A., AUMAITRE, O., ARDID, D., FIALIP, J. & DUCHENE-MARULLAZ, P. (1991). Long-lasting antinociceptive effect of RC-160, a somatostatin analog, in mice and rats. *Eur. J. Pharmacol.,* **199,** 119–121.

FIELDS, H.L. & BASBAUM, A.I. (1999). Central nervous system mechanisms of pain modulation. In: *Textbook of Pain,* eds. Wall, P.D. & Melzack, R. pp. 309–329. Edinburgh: Churchill Livingston.

HELMCHEN, C., FU, Q.G. & SANDKUHLER, J. (1995). Inhibition of spinal nociceptive neurons by microinjections of somatostatin into the nucleus raphe magnus and the midbrain periaqueductal gray of the anesthetized cat. *Neurosci. Lett.,* **187,** 137–141.

HELYES, Z., PINTER, E., NEMETH, J., KERI, G., THAN, M., OROSZI, G., HORVATH, A. & SZOLCSANYI, J. (2001). Anti-inflammatory effect of synthetic somatostatin analogues in the rat. *Br. J. Pharmacol.,* **134,** 1571–1579.

HELYES, Z., THAN, M., OROSZI, G., PINTER, E., NEMETH, J., KERI, G. & SZOLCSANYI, J. (2000). Anti-nociceptive effect induced by somatostatin released from sensory nerve terminals and by synthetic somatostatin analogues in the rat. *Neurosci. Lett.,* **278,** 185–188.

HEPPELMANN, B. & PAWLAK, M. (1997). Inhibitory effect of somatostatin on the mechanosensitivity of articular afferents in normal and inflamed knee joints of the rat. *Pain,* **73,** 377–382.

HERLITZE, S., GARCIA, D.E., MACKIE, K., HILLE, B., SCHEUER, T. & CATTERALL, W.A. (1996). Modulation of Ca^{2+} channels by G-protein $\beta\gamma$ subunits. *Nature,* **380,** 258–262.

HERVIEU, G. & EMSON, P.C. (1998). The localization of somatostatin receptor 1 (sst1) immunoreactivity in the rat brain using an N-terminal specific antibody. *Neuroscience,* **85,** 1263–1284.

HOYER, D., BELL, G., BERELOWITZ, M., EPELBAUM, J., FENIUK, W., HUMPHREY, P., O'CARROLL, A., PATEL, Y., SCHONBRUNN, A., TAYLOR, J. & REISINE, T. (1995). Classification and nomenclature of somatostatin receptors. *Trends Pharm. Sci.,* **16,** 86–88.

IKEDA, S.R. (1996). Voltage-dependent modulation of N-type calcium channels by G-protein $\beta\gamma$ subunits. *Nature,* **380,** 255–258.

KIM, C.J., RHEE, J.-S. & AKAIKE, N. (1997). Modulation of high-voltage activated Ca^{2+} channels in the rat periaqueductal grey neurons by μ-type opioid agonist. *J. Neurophysiol.,* **77,** 1418–1424.

OSBORNE, P.B., VAUGHAN, C.W., WILSON, H.I. & CHRISTIE, M.J. (1996). Opioid inhibition of rat periaqueductal grey neurones with identified projections to rostral ventromedial medulla *in vitro*. *J. Physiol. (London),* **490,** 383–389.

PINTER, E., HELYES, Z., NEMETH, J., PORSZASZ, R., PETHO, G., THAN, M., KERI, G., HORVATH, A., JAKAB, B. & SZOLCSANYI, J. (2002). Pharmacological characterisation of the somatostatin analogue TT-232: effects on neurogenic and non-neurogenic inflammation and neuropathic hyperalgesia. *N-S Arch. Pharmacol.,* **366,** 142–150.

SANDKUHLER, J., FU, Q.G. & HELMCHEN, C. (1990). Spinal somatostatin superfusion *in vivo* affects activity of cat nociceptive dorsal horn neurons: comparison with spinal morphine. *Neuroscience,* **34,** 565–576.

SCHINDLER, M., HUMPHREY, P.P. & EMSON, P.C. (1996). Somatostatin receptors in the central nervous system. *Prog. Neurobiol.,* **50,** 9–47.

SCHINDLER, M., SELLERS, L.A., HUMPHREY, P.P. & EMSON, P.C. (1997). Immunohistochemical localization of the somatostatin SST2(A) receptor in the rat brain and spinal cord. *Neuroscience,* **76,** 225–240.

SELMER, I., SCHINDLER, M., ALLEN, J.P., HUMPHREY, P.P. & EMSON, P.C. (2000). Advances in understanding neuronal somatostatin receptors. *Reg. Peptides,* **90,** 1–18.

TADDESE, A., NAH, S.Y. & MCCLESKEY, E.W. (1995). Selective opioid inhibition of small nociceptive neurons. *Science,* **270,** 1366–1369.

VAUGHAN, C.W. & CHRISTIE, M.J. (1997a). Presynaptic inhibitory action of opioids on synaptic transmission in the rat periaqueductal grey *in vitro*. *J. Physiol. (London),* **498,** 463–472.

VAUGHAN, C.W., CONNOR, M., BAGLEY, E.E. & CHRISTIE, M.J. (2000). Actions of cannabinoids on membrane properties and synaptic transmission in rat periaqueductal grey neurons *in vitro*. *Mol. Pharmacol.,* **57,** 288–295.

VAUGHAN, C.W., INGRAM, S.L. & CHRISTIE, M.J. (1997b). Actions of the ORL1 receptor ligand nociceptin on membrane properties of rat periaqueductal grey neurons *in vitro*. *J. Neurosci.,* **17,** 996–1003.

VAUGHAN, C.W., INGRAM, S.L., CONNOR, M.A. & CHRISTIE, M.J. (1997c). How opioids inhibit GABA-mediated neurotransmission. *Nature,* **390,** 611–614.

ZAMPONI, G.W. & SNUTCH, T.P. (1998). Decay of prepulse facilitation of N type calcium channels during G Protein inhibition is consistent with binding of a single G($\beta\gamma$) subunit. *Proc. Natl. Acad. Sci. U.S.A.,* **95,** 4035–4039.

(Received March 9, 2004
Revised April 30, 2004
Accepted May 25, 2004)